2012

Modular Simulation of Vapour Compression Systems With an Object Oriented Tool

Nicolas Ablanque
quim@cttc.upc.edu

Carles Oliet

Joaquim Rigola

Oriol Lehmkuhl

Carlos D. Pérez-Segarra

Modular Simulation of Vapour Compression Systems with an Object-Oriented Tool

Nicolas ABLANQUE[1*], Carles OLIET[1], Joaquim RIGOLA[1], Oriol LEHMKUHL[2], Carlos D. PEREZ-SEGARRA[1]

[1] Centre Tecnològic de Transferència de Calor (CTTC), Universitat Politècnica de Catalunya (UPC),
Colom 11, 08222 Terrassa (Barcelona), Spain. FAX: +34-93-739.89.20; Tel. +34-93-739.81.92
E-mail: cttc@cttc.upc.edu Web page: www.cttc.upc.edu

[2] Termo Fluids S.L.,
Magí Colet 8, 08204 Sabadell (Barcelona), Spain.
E-mail : termofluids@termofluids.com

ABSTRACT

The objective of this work is to simulate vapour compression refrigeration systems through a modular approach by means of an object-oriented numerical tool called NEST. For this purpose, the global system is modeled as a collection of different elements which are linked between them. Each element represents a specific part of the system (e.g. heat exchanger, compressor, expansion device, tube, cavity, wall, etc.) and can be independently solved for given boundary conditions. The global resolution procedure is carried out by solving all the elements iteratively, transferring information between them, until a converged solution is reached. The system is easily modified by adding, subtracting or substituting any of its elements. This feature gives great flexibility to the model, not only because the configuration of the system can be clearly altered, but also because the numerical model of any element can be easily replaced allowing different levels of simulation. In this work the object-oriented methodology together with the elements description and their resolution procedures are presented. The model is validated against experimental data obtained from a refrigeration cycle working with isobutane. In addition to this, an illustrative case is presented in order to show the system capabilities.

1. INTRODUCTION

Vapour compression systems are widely used to provide mechanical cooling in a wide variety of applications such as food processing, cold storage, refrigeration at different levels (domestic, medical, industrial, commercial, transport, cryogenic), air conditioning (in vehicles and public or private enclosed spaces), electronic cooling, oil refineries and chemical processing plants. These systems have been widely studied since their first appearance but nowadays they are facing new challenges due to the mankind concern in preserving the environment. Therefore the need for having more reliable and flexible tools to simulate and predict their thermal and fluid-dynamic behavior is increasing.

The work presented in this document is addressed to the implementation and development of a flexible simulation tool to study vapour compression refrigeration systems. The approach of the numerical procedure presented herein is based on a modular strategy where all the system components are considered as independent entities. These elements are linked between them so that a specific system is defined by both its elements and links. The global resolution procedure is carried out by solving all the elements and transferring information between them in an iterative way. Elements of the system may be easily added, subtracted or substitute in order to change the system configuration or to use a different simulation model for a particular element.

This paper is divided into five sections. The second section of this work is devoted to explain the modular approach. The third section presents briefs descriptions of the numerical models used to simulate the system elements (e.g. heat exchangers, compressor, expansion device, etc.). In the fourth section the model results are compared against experimental data and an additional illustrative case is also presented. Finally, in the fifth section conclusions are given.

2. MODULAR APPROACH

The modular approach consists in dividing a whole system into discrete elements. Each element can be independently solved from a set of given boundary conditions. However, the whole system resolution is done iteratively by solving all its elements and transferring the appropriate information between them. The object-oriented numerical tool called NEST used for this purpose has already been applied to energy balances in buildings (Damle *et al*. 2011a) and hermetic reciprocating compressors (Damle *et al*. 2011b).

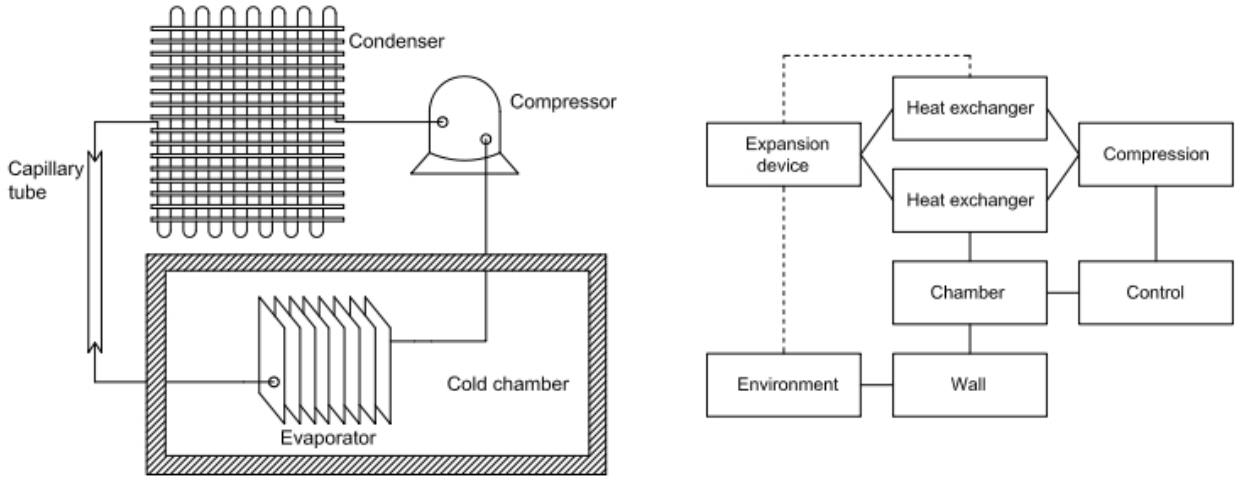

Figure 1: Refrigeration system: simplified scheme (left) and block diagram (right)

In this work the modular approach is applied to thermal systems and specifically to vapour compression refrigeration systems. In Figure 1 the simplified scheme of a refrigeration cycle with a cold chamber is presented together with the corresponding block diagram used for its modular resolution. It is observed that each component of the cycle is represented by a discrete element in the block diagram. For instance the inside of the cold chamber is simulated by a numerical routine called "chamber" which is linked to three other numerical routines: i) the "wall" which simulates the heat transfer through the insulation layer, ii) the "heat exchanger" which simulates the heat transfer and fluid-dynamic phenomena through a heat exchanger, and iii) the "control" routine which sets the compressor frequency according to the chamber temperature.

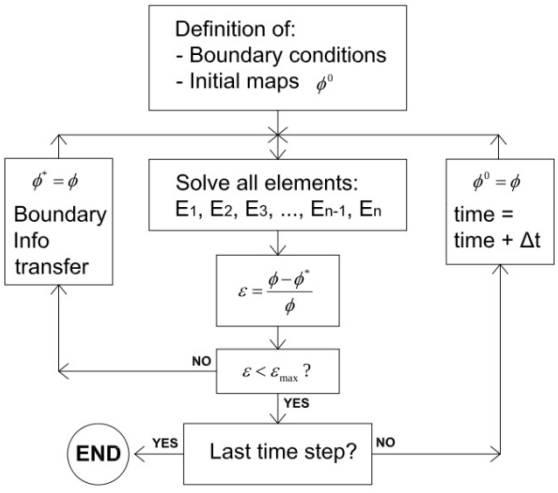

Figure 2: System global resolution algorithm

This working methodology allows adding, subtracting and substituting elements in order to represent a different system configuration or to simulate any of its elements with a different numerical model. For instance, the selection of the element used to simulate a heat exchanger will depend on the studied device but it may vary from a simple ε-NTU approach to a distributed model considering two-phase flows or to any other model with a higher level of complexity.

The global resolution algorithm is depicted in Figure 2. Initially, the input values needed for each element are obtained from the information transmitted by its neighbours. Then, the governing equations of each element are solved and new outputs are obtained. Iterations continue until convergence is reached at a given time step. From then on, further iterations are carried out for the next time steps.

3. NUMERICAL MODELS OF ELEMENTS

In this section the numerical models used by the system elements are briefly described. The heat exchangers are solved with a distributed model where the secondary fluid can be both a concentric annular flow (double-tube heat exchanger) or a fluid flow through fins (fin-and-tube heat exchanger), the compressor is simulated from a simplified formulation based on efficiencies, the expansion device is a capillary tube and its behavior is predicted by means of a numerical procedure applied to a two-phase flow model, the chamber simulation considers a unique control volume, and the wall element calculates the heat transfer through the insulation layer.

3.1 Compressor

The compressor model is based on the work by Ndiaye and Bernier (2010). A simplified scheme of the compressor is shown in Figure 3 where three main parts are considered (shell internal volume, compression chamber and discharge line). The incoming gas enters into the shell through the suction line (*suc*), then once inside the shell (*c*), it goes into the compression chamber where the compression process takes place (*in-out*), and finally the gas is expelled through the discharge line (*out-dis*).

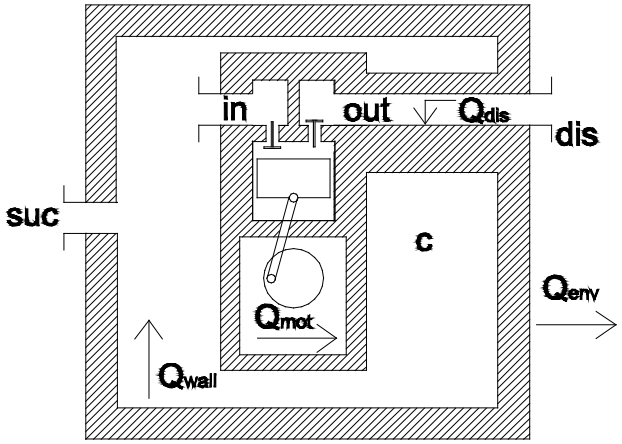

Figure 3: Simplified scheme of a hermetic compressor

The following mass and energy balances apply for the gas inside the shell (Equations 1 and 2, respectively):

$$\frac{d\rho_c}{dt}V_c = \dot{m}_{suc} - \dot{m}_{in} \tag{1}$$

$$\frac{d\rho_c h_c}{dt}V_c = \dot{m}_{suc}h_{suc} - \dot{m}_{in}h_c + \dot{Q}_{wall} + \frac{dp_c}{dt}V_c \tag{2}$$

While the energy balance over the compressor solid parts is expressed as follows (Equation 3):

$$mc_p \frac{dT_w}{dt} = \dot{Q}_{dis} + \dot{Q}_{mot} - \dot{Q}_{wall} - \dot{Q}_{env} \quad (3)$$

The model is fed with empirical heat transfer coefficients used to predict the heat transferred to/from the compressor shell. It is worth to mention some of the model more important hypotheses: the oil effects are neglected, the whole compressor metallic parts are at the same temperature, the mass flow rate through the compression chamber is equal to the mass flow rate through the discharge line, the suction pressure is equal to the pressure inside the shell, the suction and discharge mufflers influence is not taken into account, the mixture inside the shell is considered thermally homogeneous. In addition to the model equations, the compressor is characterized by both the volumetric efficiency ($\eta_v = \dot{m}/\rho V_{sw} N$) and the isentropic efficiency ($\eta_s = \dot{W}_s/\dot{W}_{cp}$). These efficiencies are also expressed by means of the compression pressure ratio and the operating frequency (the mathematical relations are obtained from experimental tests or numerical simulations previously carried out).

3.2 Heat Exchangers

The thermal and fluid-dynamic behavior of flows inside tubes is predicted with a two-phase fluid flow model based on the work by García-Valladares *et al.* (2004). The fluid domain is represented by means of consecutive control volumes where the governing equations of continuity, momentum and energy are applied and solved (Equations 4, 5 and 6, respectively):

$$\frac{d\overline{m}}{dt} + \dot{m}_i = \dot{m}_{i-1} \quad (4)$$

$$\frac{d\overline{m}\bar{v}}{dt} + \dot{m}_{g,i} v_{g,i} + \dot{m}_{l,i} v_{l,i} - \dot{m}_{g,i-1} v_{g,i-1} - \dot{m}_{l,i-1} v_{l,i-1} = (p_{i-1} - p_i) S - \bar{\tau} \pi D \Delta z_i - mg sin\theta \quad (5)$$

$$\frac{d\overline{m}(h + \bar{e}_c + \bar{e}_p)}{dt} + \dot{m}_i (h + e_c + e_p)_i - \dot{m}_{i-1} (h + e_c + e_p)_{i-1} = \dot{Q}_{wall} + V \frac{dp}{dt} \quad (6)$$

The flow is evaluated on the basis of a step-by-step numerical implicit scheme where the wall temperature map acts as the boundary condition. The formulation requires the use of empirical correlations to evaluate the void fraction (ε), the shear stress ($\bar{\tau}$) and the convective heat transfer coefficient used to evaluate the heat transferred between the tube and the fluid ($\dot{Q}_{wall}$).

3.2.1 Double tube heat exchangers: In the case of double tube counter-flow heat exchangers, the secondary fluid flow is solved with the same two-phase flow model. Here, the solid parts (including insulation layers) are discretized with a two-dimensional mesh where an energy balance is calculated. More details are found in Morales *et al.* (2009).

3.2.2 Fin-and-tube heat exchangers: For fin-and-tube heat exchangers different levels of simulation could be considered. First, the detailed model called CHESS (Oliet *et al*. 2002) where the domain is divided into a set of control volumes as fin-and-tube blocks. The model allows steady and unsteady analysis, flexible geometry and circuitry, working at dry or wet/frosting conditions. The inner refrigerant flow is solved with the two-phase flow model where non-uniform heat transfer coefficients can be considered in radial and axial directions (Oliet *et al.* 2010). Second, a ε-NTU based (steady, multi-zone) fin-and-tube heat exchanger model is also available (quickCHESS), considering dry and wet airside conditions, and evaporation/condensation for the refrigerant (Oliet *et al.* 2007).

3.3 Expansion device

The algorithm to simulate the capillary tube is based on the distributed model presented in the previous Section. The resolution procedure is carried out in two steps. The first step consists in determining if the capillary tube is working at critical or non-critical conditions, while the second consists in performing the simulation according to the condition. More details of this model are found in Ablanque *et al.* (2010).

3.3.1 Critical condition determination: The mass flow rate inside a capillary tube increases as the evaporating temperature decreases (lower discharge pressure) but only up to a critical value from which the mass flow rate

remains constant. This critical limit occurs when the entropy generation equation (see Equation 8) is not anymore accomplished ($s_{gen,i} < 0$):

$$\dot{m}_{i-1}s_{i-1} + \dot{m}_i s_i - \frac{\bar{\dot{q}}_i}{T_{wall}}\pi D \Delta z_i = \dot{s}_{gen,i} \quad (8)$$

Alternatively this limit can be calculated when *dp/dz* approaches to infinity (or $dz/dp < \varepsilon$). Therefore, when the latter equation is not accomplished at the capillary tube outlet end (last control volume) critical conditions are met (i.e. critical mass flow rate and discharge pressure). It is convenient to use a non-uniform grid for the fluid domain discretization due to the high pressure gradients.

3.3.2 Critical and non-critical flow resolution: The flow is critical when the critical discharge pressure is higher than the actual discharge pressure and non-critical in the opposite case. If the flow is non-critical new iterations are carried out in order to find the refrigerant thermal and fluid-dynamic behavior taking into account the actual discharge pressure. However, if the flow is critical, an additional control volume is considered at the capillary tube outlet end. There, an energy balance is applied to calculate the capillary tube discharge enthalpy (heat transfer and transient terms are neglected).

3.4 Additional elements

Additional elements have been used in the simulations carried out in this work (see block diagram in Figure 1). For instance, to simulate a cold chamber in a refrigeration system two main elements are used: the chamber element which consists in one node control volume where energy and mass balances are calculated, and the wall element which calculates heat conduction through walls and heat convection between walls and surroundings. These two elements can be linked to other elements in order to simulate several aspects of the cold chamber such as heat radiation exchange, fluid flow through wall openings, multiple material layers in walls, etc. Apart from this, the environment element is used to define and calculate the ambient conditions while the control element could be use to modify any variable of any element from any other variable (e.g. set the compressor working frequency according to the cold chamber mean temperature).

4. NUMERICAL RESULTS

4.1 Numerical simulation against experimental data

An experimental facility specially designed to test vapour compression refrigeration cycles has been used to obtain relevant measurements in order to validate the modular resolution model. The facility included a main loop made up of the following elements: a replaceable compressor (in this work a commercial compressor for R600a is used), a capillary tube, and two double-pipe heat exchangers. The unit was equipped with several measuring instruments along both the main loop and the auxiliary circuits.

The system numerical results were compared against experimental data obtained at transient state conditions. For this simulation, only four types of elements have been used: the two-phase flow distributed model (to simulate both heat exchangers), the compressor element, the capillary tube element and the control element (to set the compressor working frequency).

The studied case considers a variable speed compressor. The experimental test used for this goal has been carried out in one single run but varying the compressor frequency (the compressor speed has been progressively decreased from 1.25f to 0.5f Hz during the whole run by 0.25f Hz every half our – where f is the frequency value of reference). The run began at steady state with the following experimental conditions: compressor speed 1.25f Hz, refrigerant mass flow rate 2.511 kg/h, system high pressure 7.76 bar, system low pressure 0.77 bar.

Figure 4 (left) shows the evolution of the system power consumption where the numerical trends coincide with the experimental ones. The energy consumption is slightly underestimated by the numerical model for the three first working frequencies. It is worth to mention that the peak observed at every frequency change is well reproduced by the numerical model (see the zoom box of the power evolution plot). Figure 4 (right) shows the experimental and numerical results for the system low pressure evolution. The pressure is overestimated at high frequencies (1.25f and 1f Hz) and underestimated at low frequencies (0.75f and 0.5f Hz). Reasonable agreement has been observed as discrepancies were lower than 10%.

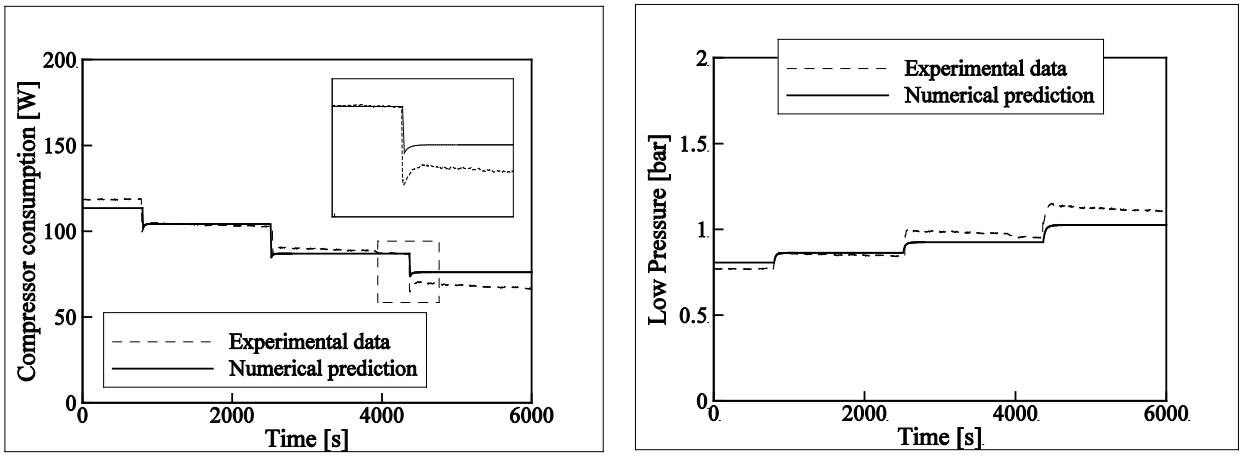

Figure 4: Refrigeration system evolution: power consumption (left) and low pressure (right)

This case represents a preliminary validation step as more comparisons must be done in order to attain a solid validation process. However, although some discrepancies between predictions and experimental data should be still improved, good general trends were observed in the simulations.

4.2 Illustrative Case

The system tackled in this section is oriented to study refrigerators with variable speed compressor (the scheme is shown in Figure 1). Regarding the validation case presented in the previous section new features are included in the system such as air-to-refrigerant heat exchangers and refrigerated rooms. The studied system starts from a global steady state situation where the compressor is working at 0.5f Hz and the mean temperature inside the cold chamber is -18 ºC. At this point, a sudden rise of 5ºC in the chamber temperature is numerically forced and the control system is activated in order to set a new compressor frequency and drive the room temperature back to -17.75 ºC. Three different responses have been evaluated: the compressor keeps working at 0.5f Hz (run 1), the compressor frequency increases progressively from 0.25f Hz to 1.25f Hz by 0.25f Hz every five minutes (run 2), and the compressor frequency makes a sudden change from 0.5f Hz to 1.25f Hz (run 3).

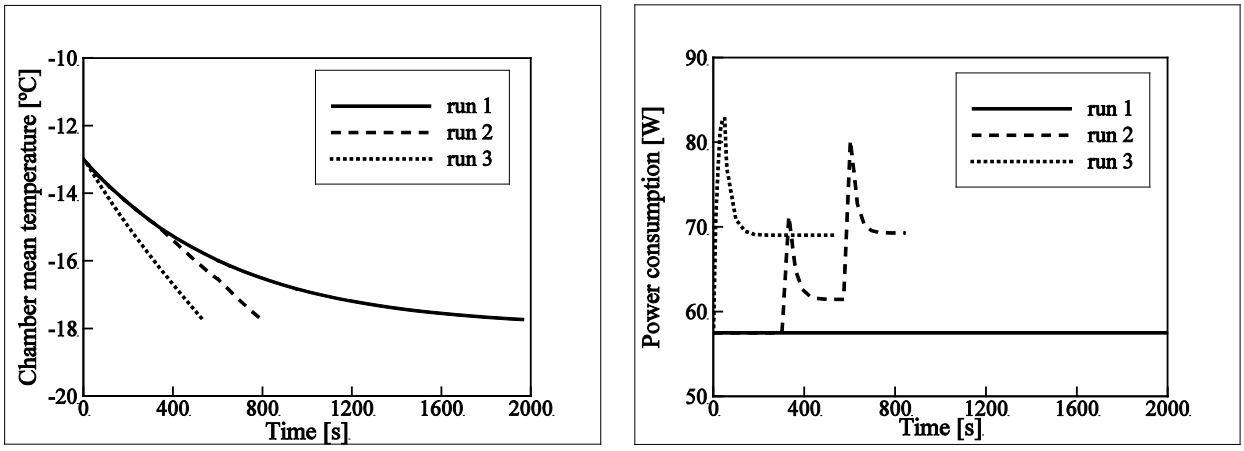

Figure 5: Refrigeration system evolution: cold chamber temperature (left) and power consumption (right)

Figure 5 (left) shows the evolution of the cold chamber temperature for the three runs (cases stop when the temperature reaches -17.75 ºC). As expected the fastest response is obtained by run 3 where the compressor is working at its maximum frequency from the beginning while the slowest response is that of run 1. Figure 5 (right) shows the compressor power consumption evolution. It is observed that the power consumption is higher for greater working frequencies and that a peak is present at the precise moment where a frequency change occurs. Table 1 shows the cooling time, the compressor energy consumption (energy spent during cooling time), and the energy consumption during 2040 seconds (this value includes the cooling energy consumption and the additional energy consumed before attaining 2040 seconds for runs 2 and 3). The latter value is presented for comparative purposes and considers that the compressor works at 0.5f after cooling time.

Table 1: Numerical results for the three tested runs

	Frequency [Hz]	Cooling time [s]	Energy consumption (cooling time) [J]	Total E. Consumption(2040 s) [J]
1	0.5f*	2040	117263	117263
2	0.5f / 0.75f / 1f / 1.25f	840	53462	122438
3	1.25f	540	37943	124163

* f - Frequency value of reference

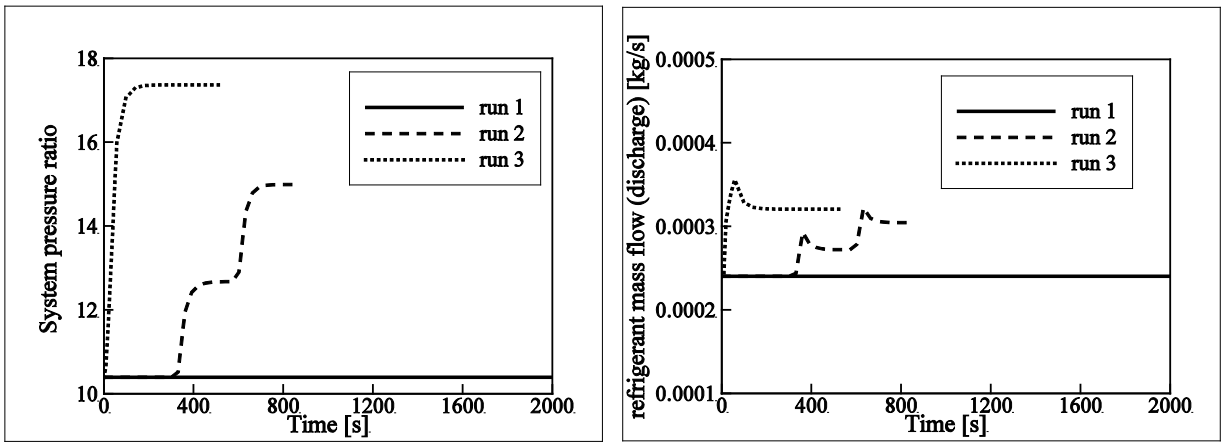

Figure 6: Refrigeration system evolution: pressure ratio (left) and mass flow rate (right)

The system pressure ratio evolution is depicted in Figure 6 (left). Higher compression ratios are observed as the working frequency is increased. The mass flow rate evolution at the discharge line is shown in Figure 6 (right). It is noticed that as the compressor frequency increases the mass flow rate increases (a peak is observed at every change of frequency).

5. CONCLUSIONS

The numerical object-oriented tool called NEST has been successfully used to solve vapor compression refrigeration systems. The model flexibility has been observed as different elements have been used in this work and two different types of configurations (system with cold chamber and without it). The model has been validated against experimental data obtaining general good agreement (discrepancies lower than 10%). An illustrative case for a transient simulation in refrigeration system has been simulated and the results were used to show the model capabilities.

NOMENCLATURE

c_p	Specific heat	(J kg^{-1} K^{-1})	S	Cross section	(m^2)
D	diameter	(m)	T	temperature	(K)
e	Specific energy	(J kg^{-1})	t	time	(s)
f	Frequency of reference	(Hz)	V	volume	(m^3)
h	specific enthalpy	(J kg^{-1})	v	velocity	(m s^{-1})

m	mass	(kg)	**greek**		
$\dot{m}$	mass flow rate	(kg s^{-1})	Δt	time step	(s)
p	pressure	(Pa)	ε	convergence criteria	(-)
$\dot{Q}$	heat	(W)	θ	angle	(rad)
s	Specific entropy	(J kg^{-1} K^{-1})	ρ	density	(kg m^{-3})
$\dot{s}_{gen}$	Generation of entropy	(J K^{-1} m^{-3} s^{-1})	φ	variable	(-)

REFERENCES

Ablanque N., Rigola J., Pérez-Segarra C.D., Oliva A., 2010. Numerical simulation of capillary tubes. Application to domestic refrigeration with isobutene. *Proceedings of the 13th International Refrigeration and Air Conditioning Conference at Purdue*. West Lafayette, p. 1-8.

Damle R., Lehmkuhl O., Colomer G., Rodriguez I., 2011a. Energy simulation of buildings with a modular object-oriented tool. *Proceedings of the ISES Solar World Congress*. Kassel, Germany, p. 1-11.

Damle R., Rigola J., Pérez-Segarra C.D., Castro J., Oliva A., 2011b. Object-oriented simulation of reciprocating compressors: Numerical verification and experimental comparison. *International Journal of Refrigeration* 34 (8), p. 1989-1998.

García-Valladares O., Pérez-Segarra C.D., Rigola J., 2004. Numerical simulation of double-pipe condensers and evaporators. *International Journal of Refrigeration* 27 (6), p. 656-670.

Morales-Ruiz S., Rigola J., Pérez-Segarra C.D., García-Valladares O., 2009. Numerical analysis of two-phase flow in condensers and evaporators with special emphasis on single-phase/two-phase transition zones. *Applied Thermal Engineering* 29 (5-6), p. 1032-1042.

Ndiaye D., Bernier M., 2010. Dynamic model of hermetic reciprocating compressor in on-off cycling operation. *Applied Thermal Engineering* 30, p. 792-799.

Oliet C., Pérez-Segarra C.D.,Castro J., Oliva A., 2010. Modelling of fin-and-tube evaporators considering non-uniform in-tube heat transfer.*International Journal of Thermal Sciences* 49 (4), p. 692-701.

Oliet C., Pérez-Segarra C.D.,Danov S., Oliva A., 2007. Numerical simulation of dehumidifying fin-and-tube heat exchangers: Semi-analytical modeling and experimental comparisons. *International Journal of Refrigeration* 30, p. 1266-1277.

Oliet C., Pérez-Segarra C.D.,Danov S., Oliva A., 2002. Numerical simulation of dehumidifying fin-and-tube heat exchangers. Model strategies and experimental comparisons. *Proceedings of the Int. Refrigeration Engineering Conference.* Purdue, US, p. 1-8.

ACKNOWLEDGEMENT

This work has been developed within the project “Innpacto KERS” (IPT-02000-2010-30) between the company Fagor Electrodomésticos, S. Coop. and the CTTC, and within the projects ENE2011-28699 + ENE2009-07689 of the Spanish government (“MINECO, Secretaría de Estado de Investigación, Desarrollo e Innovación”).